Journal of Colloid and Interface Science 580 (2020) 439–448

Contents lists available at ScienceDirect

Journal of Colloid and Interface Science

journal homepage: www.elsevier.com/locate/jcis

Kinetics of the thermal response of poly(N-isopropylacrylamide co methacrylic acid) hydrogel microparticles under different environmental stimuli: A time-lapse NMR study

Marta Martinez-Moro [a], Jacek Jenczyk [b,*], Juan M. Giussi [c], Stefan Jurga [b], Sergio E. Moya [a,*]

[a] Center for Cooperative Research in Biomaterials (CIC biomaGUNE), Basque Research and Technology Alliance (BRTA), Paseo de Miramon 182 C, 20014 Donostia-San Sebastian, Spain
[b] NanoBioMedical Centre, Adam Mickiewicz University, Wszechnicy Piastowskiej 3, 61-614 Poznań, Poland
[c] Instituto de Investigaciones Fisicoquímicas Teóricas y Aplicadas (INIFTA), Departamento de Química, Facultad de Ciencias Exactas, Universidad Nacional de La Plata, CONICET, La Plata 1900, Argentina

GRAPHICAL ABSTRACT

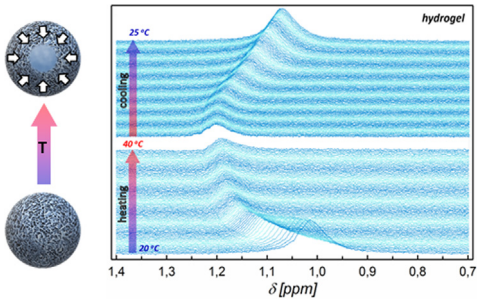

ARTICLE INFO

Article history:
Received 25 March 2020
Revised 8 July 2020
Accepted 10 July 2020
Available online 15 July 2020

Keywords:
Time-lapse NMR
NIPAM-MAA microgels
Hydrogel collapse
Deswelling kinetics
Polyamines

ABSTRACT

Hypothesis: Hydrogels of N-isopropylacrylamide and methacrylic acid (P(NIPAm-*co*-MAA)) display pH sensitivity and complex positively charged molecules through carboxylate groups, while having a critical solution temperature at which they reduce in volume and dehydrate. We aimed to elucidate how the responsiveness of MAA to environmental changes alters PNIPAm hydrogels at the molecular level using nuclear magnetic resonance (NMR). Time-lapse NMR allows us to follow the evolution of NMR signal under a temperature stimulus, providing unique information on conformational freedom of the hydrogel polymers.

Experiments: We used time-lapse NMR to follow the evolution of the NMR signal with time over a temperature change from 25 to 40 °C and to study the swelling/deswelling kinetics of P(NIPAm-*co*-MAA) microgels at different pH values and ionic strengths, and in the presence of positively charged molecules complexing carboxylate groups.

Findings: At acid pH, hydrogel collapse is favored over neutral pH, and at basic pH the carboxylates remain steadily hydrated during temperature increase. Increasing ionic strength results in a faster, more effective collapse than decreasing pH. Complexation of medium-sized molecules with several charges

Abbreviations: APS, ammonium persulfate; BIS, N,N'-methylene-bis-acrylamide; DLS, dynamic light scattering; HCl, hydrochloric acid; LCST, lower critical solution temperature; MAA, methacrylic acid; MW, molecular weight; NaCl, sodium chloride; NaOH, sodium hydroxide; NIPAM, N-isopropylacrylamide; NMR, nuclear magnetic resonance; P(NIPAm-*co*-MAA), poly(N-isopropylacrylamide-*co*-methacrylic acid); PAH, polyallylamine hydrochloride; PDADMAC, polydiallyldimethylammonium chloride; SDS, sodium dodecylsulfate; T_2, spin-spin relaxation time; VPT, volume phase transition; ζ-potential, zeta potential.

* Corresponding authors.
E-mail addresses: jacjen@amu.edu.pl (J. Jenczyk), smoya@cicbiomagune.es (S.E. Moya).

https://doi.org/10.1016/j.jcis.2020.07.049
0021-9797/

(spermine, spermidine) causes a faster collapse than complexation with large molecular weight poly(allylamine) hydrochloride, but similar to the collapse effected by large poly(diallyldimethylammonium) chloride. This work opens new perspectives to using time-lapse NMR to study thermoresponsive systems that respond to multiple stimuli, with particular relevance in designing hydrogels for drug delivery.

1. Introduction

Micro- and nanometer sized hydrogels, micro(nano)gels, are colloidal particles formed by highly hydrated crosslinked polymer networks [1,2]. They are usually designed to undergo a volume phase transition (VPT) in response to specific stimuli, such as temperature, pH, ionic strength, or solvent nature. Thermoresponsive hydrogels respond to temperature turning from solution to gel. Microgels based on poly(N-isopropylacrylamide) (PNIPAm) are probably the most studied thermosensitive hydrogels. PNIPAm hydrogels exhibit a VPT at 30–32 °C, the so-called nominal lower critical solution temperature (LCST) [3]. Below this temperature the microgel particles are in a swelling (hydrated) state and the interactions monomer-solvent prevail over the monomer–monomer interactions. Above this temperature, the hydrogen bonds between the cross-linked PNIPAm chains and water break, resulting in a drastic microgel particle size decrease [4] to the deswelling (dehydrated) state. Micro- and nanogels with a transition temperature near physiological conditions have drawn increasing attention due to their potential application in sensing [5–7], regenerative medicine [8], and drug delivery [9–11].

For drug delivery applications, below LCST PNIPAm based hydrogels provide an environment suitable for the encapsulation of hydrophilic and charged drugs, since PNIPAm is highly solvated in water by hydrogen bonding interactions (although it itself is practically not charged). However, to improve the loading capacity and retention of charged drugs in PNIPAm-based microgels it is often necessary to introduce ionic co-monomers into the PNIPAm network [12,13]. Microgels formed by copolymers of PNIPAm and methacrylic acid (MAA), poly(N-isopropylacrylamide-*co*-methacrylic acid) (P(NIPAm-*co*-MAA)), retain the thermoresponsive characteristics from PNIPAm while the negative charges of MAA can complex positively charged drugs [14]. The carboxylate groups also bring pH sensitivity to the system. Small changes in pH can have a large effect on the LCST of the hydrogel. This feature can be useful for drug delivery, where physiological temperature and local pH differences can both act as stimuli to facilitate molecular switching over a desired pH range.

The presence of carboxylate groups in P(NIPAm-*co*-MAA) hydrogels can significantly alter the hydration of the hydrogel [15–17]. Indeed, carboxylate groups in MAA are known to be highly hydrated and their hydration largely depends on pH. At acidic (low) pH, the protonation of the carboxylates reduces hydration while at basic pH, hydration is increased.

The complexation of the carboxylate groups with positively charged molecules can alter their hydration, and depending on the nature of the positively charged molecules (i.e., primary amine, quaternary ammoniums, or small or large molecular weight), the effect on dehydration may be more or less pronounced. Hydration of carboxylate groups can also be affected by the ionic strength, which can screen charges in carboxylates and weaken hydrogen bonding with water. Carboxylates can also form hydrogen bonds with the NIPAm monomers, altering their hydration as well [18].

Overall, the variations in water content in the hydrogels, through the hydration of carboxylate groups triggered by changes in pH, ionic strength, or the presence of oppositely charged molecules, should affect the environment of NIPAm monomers and their thermal transition from a hydrophilic to a hydrophobic material.

Nuclear magnetic resonance (NMR) spectroscopy is one of the most powerful methods to study thermoresponsive polymers, and in particular the VPT [19]. Since NMR is very sensitive to polymer dynamics and the local chemical environment of studied nuclei, the coil-globule transition at LCST can be clearly observed in NMR spectra and it is possible to trace its evolution over time. Accordingly, comprehensive analysis of NMR data provides a thorough picture of the rearrangement of polymer chains at the molecular level, which makes this approach unique in comparison to commonly used light scattering techniques. Indeed, there are a number of studies that exemplify the exceptional efficiency of NMR methods for monitoring thermoresponsive materials [20–26]. Most of these works rely on evolution of NMR spectra as a function of temperature, measuring the spectra so that at each specific temperature there is a thermodynamic equilibrium established before actual signal acquisition takes place. Such approach proved to be very reliable for LCST determination but lacks information about the VPT kinetics.

To study the impact of the MAA groups on the phase transition of NIPAm hydrogels at the molecular level, we performed time-lapse NMR measurements [27–30], which allowed us to follow the evolution of the NMR signal over time with changes in temperature. As temperature increases over the phase transition, NIPAm dehydrates becoming a more solid-like material with limited conformational degrees of freedom. Dehydration thus leads to a decrease in the overall chain dynamics and accordingly to an increase in residual dipolar coupling. Consequently, the NMR signal decays faster due to a substantially reduced spin–spin relaxation time (T_2). A significant fraction of immobilized protons generates extremely broadened NMR signals which are beyond detection by conventional high resolution NMR probes. Therefore, eventually an apparent signal intensity drop can be observed during VPT. By tracing changes in the intensity of the NMR signal with time sweeping temperatures from 25 to 40 °C, we were able to study the kinetics of swelling and deswelling of P(NIPAm-*co*-MAA) hydrogels at different pH values and ionic strengths, and in the presence of small positively charged molecules such as doxorubicin; medium-sized oligomers like spermine and spermidine; or larger polymers such as polyallylamine hydrochloride (PAH) or polydiallyldimethylammonium chloride (PDADMAC).

Time-lapse NMR studies provide insight into the molecular changes in the P(NIPAm-*co*-MAA) hydrogel during temperature collapse and show how the presence of negatively charged and highly hydrated carboxylate groups impacts collapse at the molecular level. To our knowledge, this is the first time that time-lapse NMR has been used to study the temperature-induced collapse of a PNIPAm hydrogel co-polymerized with a second monomer, in this case MAA, that conveys additional sensitivity of the system to environmental conditions, especially pH and interactions with polyamines. Time-lapse NMR provides unique information on the polymer chain dynamics during hydrogel collapse and shows how the phase transition is affected by various environmental stimuli, which cannot be assessed by other means.

2. Experimental section

2.1. Materials

N-isopropylacrylamide (NIPAm, 97%), N,N'-methylene-bis-acrylamide (BIS, 99%), sodium dodecylsulfate (SDS), ammonium persulfate (APS, 98%), methacrylic acid (MAA, 99%), polyallylamine hydrochloride of 15 kDa (PAH 15 kDa), polyallylamine hydrochloride of 50 kDa (PAH 50 kDa), doxorubicin hydrochloride 98.0–102% (HPLC), polydiallyldimethylammonium chloride average (high molecular weight 20%wt in H_2O, PDADMAC), spermine tetrahydrochloride, spermidine trihydrochloride, sodium chloride (NaCl), hydrochloric acid (HCl),), sodium hydroxide (NaOH) and deuterium oxide (D_2O 99.8%) were purchased from Sigma Aldrich. Polyallylamine hydrochloride of 140 kDa was obtained from Alfa Aesar.

2.2. Methods

2.2.1. Microgel synthesis

P(NIPAm-*co*-MAA) hydrogels were obtained via free-radical polymerization [28,31]. In a 100 mL milliQ water solution, 16 mmol of NIPAm, 0.14 mmol SDS and 0.31 mmol of BIS were dissolved and heated up to 70℃ under magnetic stirring and N_2 bubbling during 1 h. Then, 2.12 mmol of MAA was added and stirred for 10 min. To start the reaction, 0.26 mmol of APS solution was introduced to the mixture which was kept during 3 h under magnetic stirring. Following the synthesis, hydrogels were collected by centrifugation and washed with milliQ water three times.

2.2.2. Sample preparation

In all samples the microgel concentration was 1 $mg{\cdot}mL^{-1}$ in water for DLS, or in deuterated water for NMR experiments. pH was varied by adding HCl or NaOH at 1 M in D_2O, until the desired pH was obtained. PAH, PDADMAC, spermine or spermidine were added to the hydrogel solutions at 20% of hydrogel mass. The pH was measured with a pH meter. The hydrogel solution was transferred to the NMR tubes using a syringe.

2.2.3. Dynamic light scattering (DLS)

Size and ζ-potential measurements were carried out with a Malvern ς-Sizer Nano ZS in backscattering mode at a 173° scattering angle. Measurements were made in triplicate with the temperature controlled at 25 °C and 40 °C.

2.2.4. Time-lapse NMR

Measurements were performed using an Agilent NMR 400 MHz spectrometer equipped with a double channel X{^{1}H} OneNMR probe. Spectra were acquired using simple one pulse excitation experiments with NMR signal locking. 5 mm NMR tubes were used. NMR probe temperature was monitored and controlled using a variable temperature system with ~ 0.1 °C accuracy.

NMR experiment protocol: Before the experiment was performed, the temperature inside the NMR probe was set to 40 °C (above LCST) and stabilized for at least 20 min. Dry air (dew point ~ -70 °C) was used as a heating/cooling medium. Subsequently, the fully hydrated sample, having a temperature equal to 20 °C, was transferred directly to the probe using air cushion lift. The total time required to transfer the sample to the probe (using the air cushion lift) and start acquisition was approximately equal to 0.75 s. Immediately after transfer, NMR spectra were acquired according to a predetermined time sequence. The time interval between each acquisition was 2.5 s. Short excitation pulses were applied (45°).

3. Results and discussion

3.1. DLS

Dynamic light scattering was used to trace the swelling behavior of P(NIPAm-*co*-MAA) hydrogels. Measurements at 25 °C and 40 °C were carried out to characterize the behavior of the hydrogel above and below its LCST. Increasing the temperature above the LCST causes the PNIPAm chains to dehydrate and interact with each other forming hydrophobic regions with a smaller volume than in the hydrated phase. As a consequence, the hydrogel decreases in size. However, since the density of charges from MAA often decreases too, the repulsion among hydrogel microparticles decreases, leading to their aggregation (Fig. 1a) [14,32].

Carboxylate groups in MAA are very sensitive to pH. When pH is increased, the hydrogel expands from 357 ± 10 nm to 455.6 ± 24.5 nm because at basic pH the carboxylates are more charged and hydrated (Fig. 1c). On the other hand, acid pH values result in a decrease in the hydrogel charge, water content, and size (Fig. 1b). At 25 °C and pH 2.8, the hydrogel size decreases by 22% compared with its size at pH 6.8 at the same temperature. When the temperature of the sample rises to 40 °C, the size of the hydrogel increases, possibly due to aggregation. The ionic strength also strongly affects the hydration of the carboxylates (Fig. 1d and e). When ionic strength is increased, the charges of the hydrogel are screened, which in turn decreases hydration causing hydrogel deswelling and eventually precipitation as shown for those in 500 mM NaCl (Fig. 1e).

Previously, we have studied the interaction of P(NIPAm-*co*-MAA) hydrogels with polyamines, and have shown that the interaction with polyallylamine hydrochloride (PAH) results in deswelling of the hydrogels [21]. The response of the hydrogels with PAH depends on the molecular weight (MW) of the polymer (Fig. S1, Supporting information). With the addition of 15 kDa PAH 20% in weight, the hydrogel size does not change with the temperature. The absence of changes in this case is likely due to PAH acting as an electrostatic crosslinker. PAH of this MW and at the concentration studied fully enters the hydrogel structure. Primary amines of PAH interact with the carboxylates of MAA [30]. Several carboxylate groups in the hydrogel complex with one PAH chain, which limits the hydrogel collapse. For 50 kDa PAH, in addition to the diffusion of PAH inside the hydrogel, there is also deposition of the polymer on the hydrogel surface. In these conditions, the complexation of carboxylate groups is less pronounced and the hydrogel can change size [33]. In Fig. S1 we can also observe for the microgels exposed to PDADMAC that DLS at 25 and 40 °C is practically the same, which can be interpreted as a result of PDADMAC acting as electrostatic-crosslinker. After interaction with spermidine, a low molecular weight triamine, microgels show a similar DLS behavior as PDADMAC, practically no changes in size with temperature. This behavior can again be understood as the small cationic molecule entering in the hydrogel and acting as an electrostatic-crosslinker that restricts changes in the microgel. In case of spermine, also a small cationic molecule but with four amine groups, we observe that the sizes of the hydrogels at 25 °C are smaller than for spermidine. We interpreted this as the spermine having a more dehydrating effect on the hydrogel due to a larger number of amines interacting with carboxylates. When the hydrogel with spermine collapses at 40 °C the size of the hydrogel increases as a result of additional aggregation. The response of P(NIPAm-*co*-MAA) hydrogels to environmental conditions is illustrated in Scheme 1.

3.2. Time-lapse NMR

The mechanism of the time-lapse NMR experiment relies on monitoring of the NMR spectrum evolution under specific conditions. This time-resolved strategy has been widely employed in

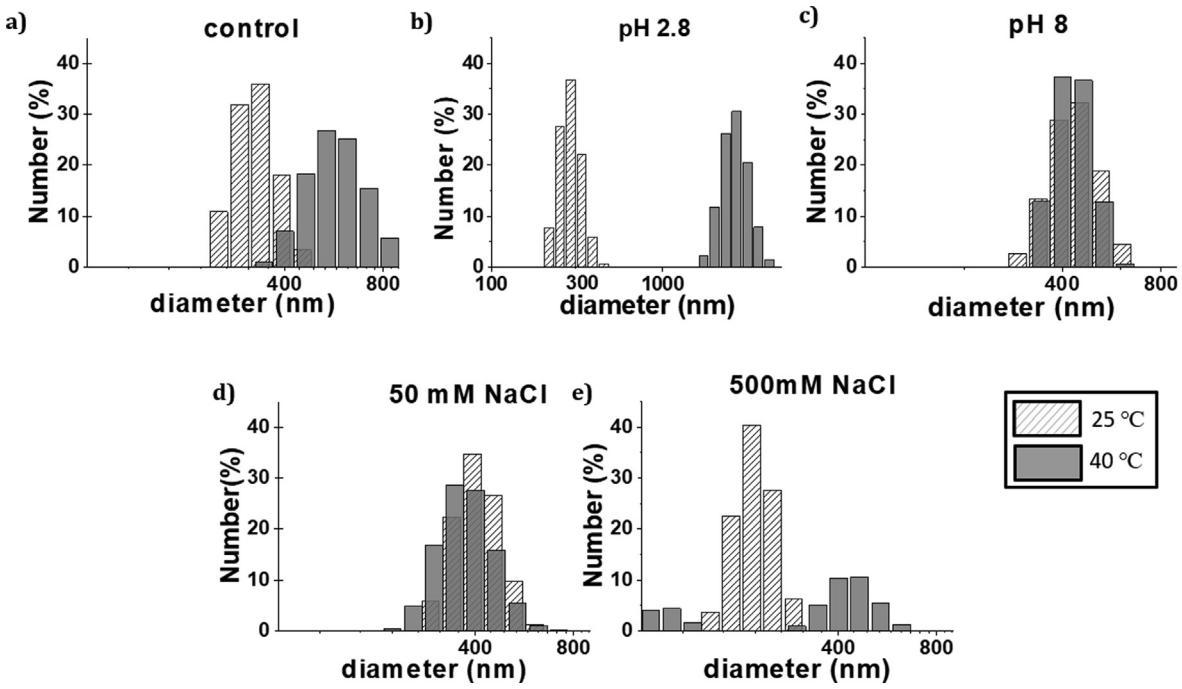

Fig. 1. Dynamic light scattering intensity distributions of hydrogels in a) water at pH 6.8, b) water at pH 2.8, c) water at pH 8, d) 50 mM NaCl, and e) 500 mM NaCl. Results for 25 °C are shown in dashed bars and for 40 °C in dark grey.

the case of *in situ* study of reaction kinetics to enhance understanding of the reaction processes [34,35]. It is a powerful method provided the time scales of the reaction are long enough to acquire a representative set of spectra displaying the kinetics of the studied process. Here, variable-temperature time-lapse NMR experiments [27–30] were conducted to obtain insight into the collapse and swelling/deswelling processes with temperature at the molecular level in P(NIPAm-*co*-MAA) hydrogels, and to investigate how swelling and deswelling are affected by the presence of carboxylates. This technique enables monitoring hydration-dehydration processes at the molecular level and tracing of their kinetics. Hydrogel VPT was analysed from the changes in the signal of methyl protons of the isopropyl group from the NIPAm monomer [36,37]. All the data presented in Figs. 4-7 are based on the NMR peak area analysis (see Supporting Information). The ^{1}H NMR spectrum of PNIPAm was recorded at room temperature (Fig. 2).

The NMR signal varies in intensity during NIPAm collapse (Fig. 3). This variation in the amplitude of the NMR signal results from a gradual stiffening of the polymer network above LCST and accompanying reduction of spin–spin relaxation time T_2. In the collapsed state the hydrogel resembles a solid-like material characterized by significantly reduced polymer dynamics. Accordingly,

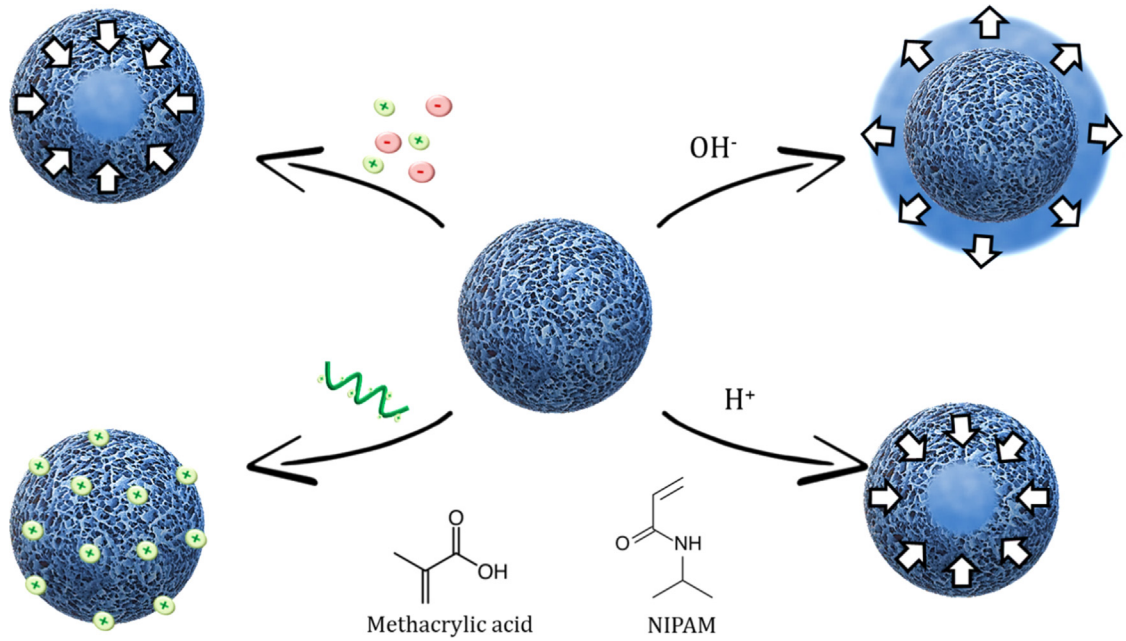

Scheme 1. Sketch of the response of P(NIPAm-*co*-MAA) hydrogels to environmental stimuli: ionic strength, pH, and presence of polyamines.

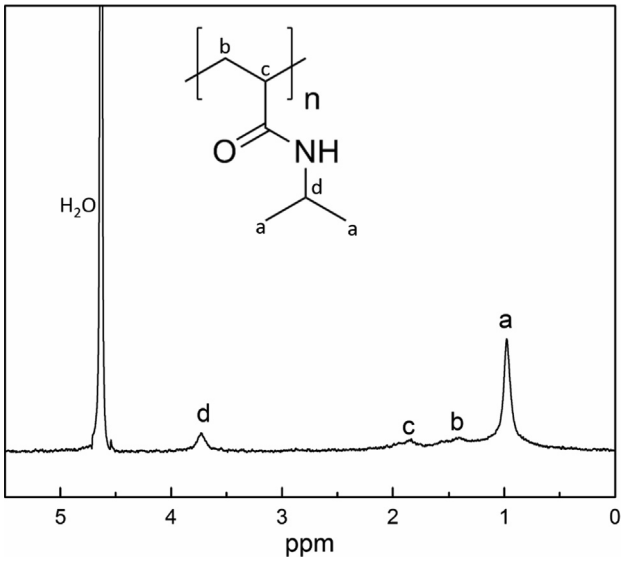

Fig. 2. PNIPAm + D_2O solution ^1H NMR spectrum recorded at room temperature. The signal from methyl protons is labelled with **a** in the spectrum.

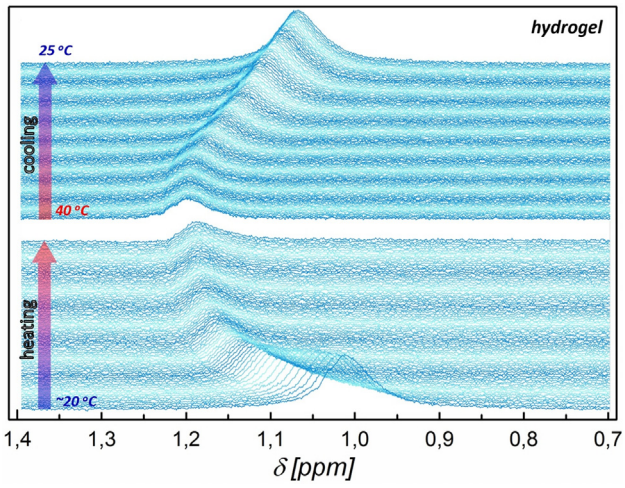

Fig. 3. Evolution of the methyl proton signal from the ^1H NMR spectra of P(NIPAm-*co*-MAA) in D_2O solution during heating and cooling experiments. The NMR signal corresponds to methyl protons from NIPAm.

the NMR free induction decay signal involves a fast decaying component, which is not fully accessible by high-resolution NMR probes. Consequently, an apparent decrease in signal amplitude takes place upon dehydration. This decrease can be employed to probe the kinetics of the VPT. To prove reversibility of dehydration-hydration processes, an additional cooling experiment was performed (Fig. 3). It is worth pointing out that the cooling experiment reveals the opposite effect of the heating experiment. Upon swelling, the intensity of the NMR signal increases indicating higher mobility of polymer chains. It is also important to emphasize that the intensity variations in NMR signal $I(t)/I_0$ observed in both cooling and heating experiments are of the same magnitude. Therefore, NMR data nicely reveal the reversibility of the VPT for the thermoresponsive gel. A chemical shift variation can also be appreciated with the variations in temperature (Fig. 3). According to Sun et al. [28], Tokuhiro et al. [36], and Tang et al. [30], this change is directly related to the deshielding effect upon VPT. Nevertheless, we believe that this specific phenomenon is predominantly related to the temperature dependance of the chemical shift of the lock signal [38], which is D_2O signal in this particular case. The software of the NMR equipment assigns a constant position to the lock signal, which results in the shift of the signal of the methyl groups (and other signals from the hydrogel), to the same extent as the D_2O shift. Therefore, the observed variation of the hydrogel signal position is solely apparent. Detailed disscusion concerning chemical shift variation is presented in the Supporting Information (Figs. S2 and S3). It is known that for the interval from 20 to 40 °C the signal of D_2O displays a linear shift with temperature of $\Delta\delta \sim 0.2$ ppm [35]. Assuming that the shift of the methyl groups mirrors that of D_2O, it is possible to estimate the temperature variations of the sample during the time-lapse experiment. It is worth mentioning that the cooling experiment is strongly affected by the significant heat capacity of the NMR probe. Therefore, the chemical shift variations recorded upon the heating and the cooling experiments do not exhibit perfect symmetry and they cannot be treated as exact 'mirror" responses. Using standard NMR probes it is not possible to perform experiments with specified heating/cooling ramps. To observe the evolution of the NMR spectra during cooling we simply switch off the heater and subsequently record the spectra until the probe reaches 25 °C. The large heat capacity of the NMR probe is manifested by the sigmoidal character of variations of the chemical shifts during cooling. In Fig. 3, the very first spectrum (bottom panel) represents the moment when the sample is just lifted down to the NMR probe and hence its temperature must be close to ~20 °C. Accordingly, subsequent spectra exhibit quite an abrupt change in chemical shifts and this change reveals an exponential character. The whole heating experiment lasted nearly 100 s. Before the cooling experiment was started, the sample remained in the probe for another several minutes. Therefore, the chemical shift observed in the very first spectrum from the cooling experiment (bottom panel) is slightly higher than the chemical shift observed for the very last spectrum from the heating experiment. In fact, the very first NMR spectrum from the cooling experiment represents the stage where the sample is already in equilibrium at 40 °C. It is shown that the total chemical shift change from ~20 °C to 40 °C equals $\Delta\delta \sim 0.2$ ppm. Assuming that our initial NMR peak position represents ~20 °C we can easily recalculate the actual temperature of the sample throughout the time-lapse experiment relying on the linear dependence between temperature and D_2O chemical shift. Since there is certain finite time (~3 to 4 s) required to transfer the sample to the probe using air cushion lift and start acquisition, the initial temperature can slightly differ from 20 °C. Therefore, in the figures representing evolution of the temperature versus time, there are error bars included of ±1 °C. This indirect temperature assessment could not be applied to the samples in 500 mM NaCl as the chemical shifts follow a different progression, which can be explained by an altered temperature dependence of the chemical shift of the solvent in the presence of a high concentration of salt. The temperature variations estimated from chemical shifts are shown for each experiment and have been included in each figure showing the $I(t)/I_0$ variations for the different experimental conditions studied, with the exception of 500 mM NaCl. In Supporting information the estimated temperature evolution has been ploted for each $I(t)/I_0$ curve (Fig. S5, S7, S8) with the exception of the experiments with NaCl where we have plotted the time evolution of the chemical shifts.

In addition, it is worth mentioning that the kinetics measured by time-lapse NMR describes the process of losing conformational freedom for the methyl groups of NIPAm, and it is not a sharp transition as observed macroscopically for NIPAm collapse. The times measured correspond indeed to the process of losing water associated to the NIPAm groups, which is likely to start before the actual temperature of collapse and extend over the collapse. We were not aiming here to record the exact phase transition temperature as

the main objective of this work, but rather the changes in polymer chain mobility for the hydrogels in response to changes in the environment. Since we can assume the same heating capacity for all the samples (same volume, mass, material) with the possible exception of the sample at 500 mM NaCl as discussed below and in supporting, and the protocol for heating/cooling is always the same, we can safely assume that the changes in the evolution of the NMR signal with time are due to the impact on the hydrogel of pH, ionic strength or presence of polyamines.

3.3. Hydrogels under different pH values

To verify the influence of pH on the thermoresponsive properties and VPT of P(NIPAm-*co*-MAA) hydrogels, time-lapse NMR experiments were conducted under different pH conditions. The results reveal that the polymer network tends to collapse rapidly under acidic conditions while remains steadily hydrated at basic pH (Fig. 4). Experiments were performed for pH values between 2.7 and 8 and the NMR spectra during deswelling at pH 2.7, 6.8 and 8 are presented as examples of acid, neutral and basic pH (Fig. 4). The $I(t)/I_0$ is also plotted for the deswelling experiments for all pH values studied and their slopes give information about the collapse kinetics. The sample at pH 6.8 is considered a control as this is the pH of the solution of hydrogels dispersed in D_2O. At this pH, the $I(t)/I_0$ decreased by 50% over 50 s, then remained constant afterwards. At pH 6.3 and 2.7, we observed a decrease of the $I(t)/I_0$ to approximately 70%. The sample at pH 2.7 shows a faster decay in intensity (slope of 0.016, Fig. 4). In this case the plateau is reached in 40 s while for the sample at pH 6.8 the plateau only appears after 50 s.

From the variation of chemical shifts of the methyl groups we were able to estimate the temperature changes of the sample with the time (Fig. 4b, Fig. 5S) and the temperature corresponding to the starting point of the plateau, which can be assumed as the phase transition temperature, the temperature at which the collapse of NIPAm monomers is complete. $I(t)/I_0$ values decrease linearly until reaching a plateau with the exception of the very first values measured, which do not seem to follow a lineal regime. The reason for the deviation of these points from lineality is probably related to the finite heat capacity of the NMR tube. Indeed, if one looks at the initial points of the curves showing the temperature evolution in the tube they seem to follow a linear regime and not the exponential trend of the rest of the temperature curve. For most of the $I(t)/I_0$ curve with the exception of the first point a lineal fiting could be applied. Points used for the lineal fitting are highlighted in Figs. S5–S8. The beginning of the plateau seems to shift to lower temperature as the acidity increases, from ~34 to ~32 °C. A small shift towards lower temperatures can be understood from a

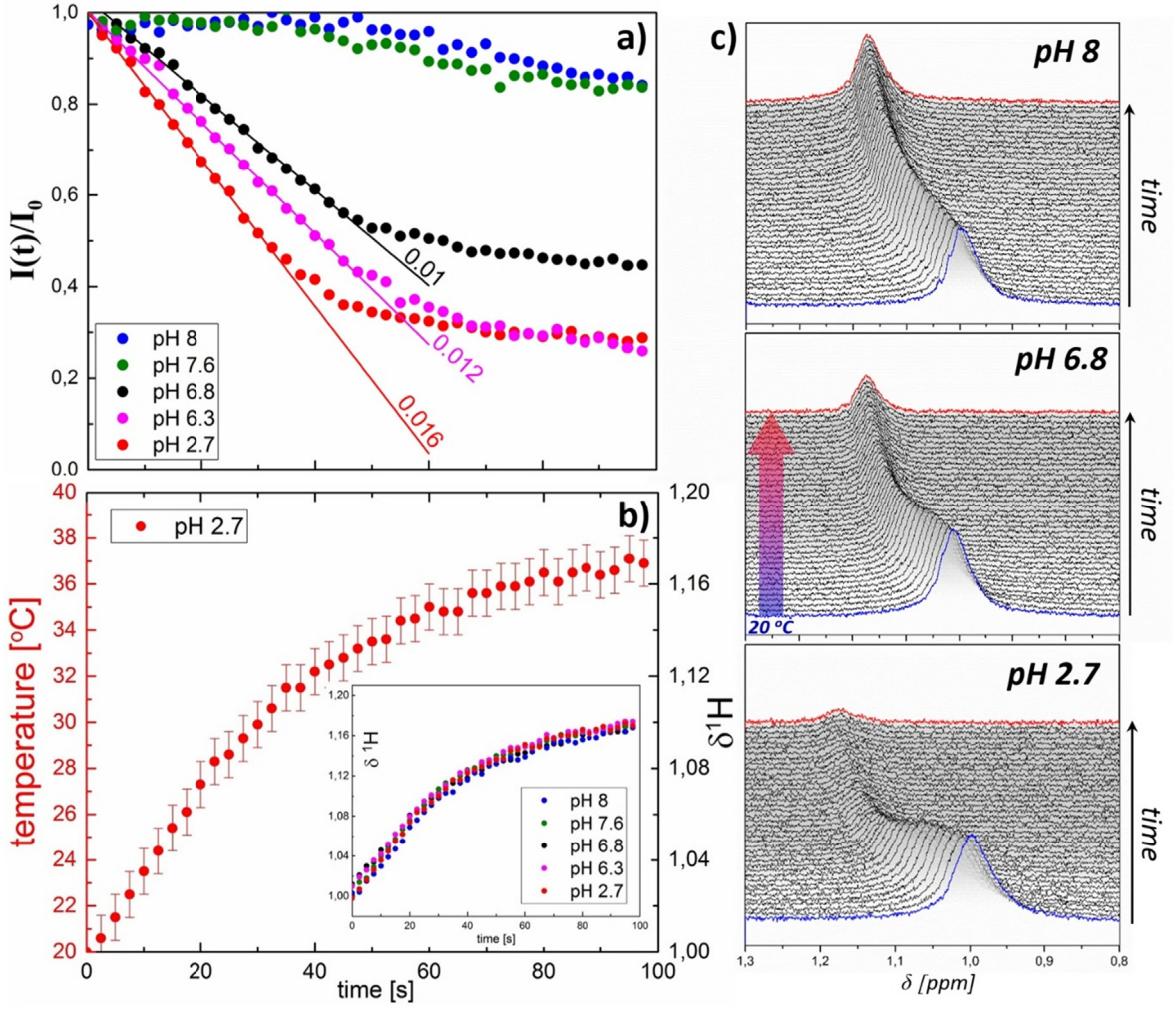

Fig. 4. Deswelling kinetics of PNIPAm microspheres under different pH conditions. a) Evolution of the $I(t)/I_0$ methyl proton signal with time for pH values from 2.7 to 8. b) Temperature of the sample versus time for the sample at pH 2.7. The inset graph represents the chemical shift variation over time for all different pH conditions. c) Change in the methyl proton NMR signal during deswelling for pH 2.7, 6.8 and 8.

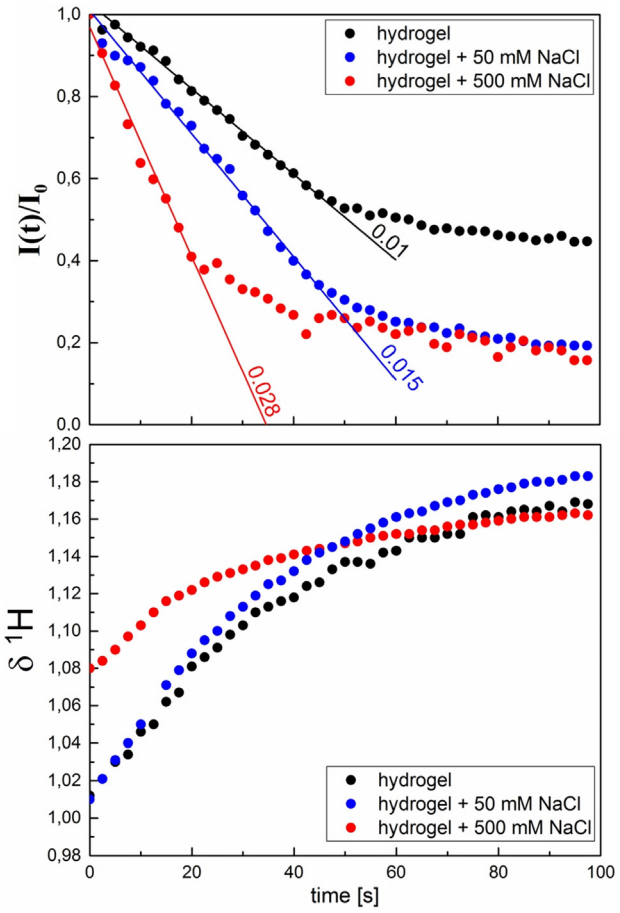

Fig. 5. Top, dehydration kinetics for PNIPAm microspheres under different ionic strengths. Dotted lines show the evolution of the $I(t)/I_0$ over time for the hydrogel alone and in the presence of 50 mM or 500 mM NaCl. Bottom, chemical shift of methyl groups in the presence of 50 and 500 mM NaCl. All experiments were recorded at pH 6.8.

decrease in the hydration of NIPAm with pH since the carboxylate groups of MAA are more protonated and can form hydrogen bonds with NIPAm themselves, altering the interaction with water of NIPAm through hydrogen bonding. Since we are looking at the relaxion of the methyl groups the shift towards lower temperatures could also be due to a decrease in the water content of the hydrogel as the carboxylates are less hydrated at lower pH. In this regard, it can be observed that the plateau is reached at lower intensities as the pH decreases. The differences in the intensities for the plateau are indicative of different levels of conformational freedom for the methyl group in each situation, and can clearly be related to the water content in the hydrogel. The plateau is reached at the lowest intensities for pH 2.7 at which the carboxylates are less hydrated and the water content of the hydrogel is lower than at higher pH values.

A completely different scenario is observed at pH 7.6 and 8. The intensity of the NMR signal remains practically constant during the whole experiment, with almost no decrease of the initial signal. This result implies that the methyl groups in PNIPAm retain their conformation dynamics as before the collapse. In other words, the methyl groups are in a hydrated environment and do not form a solid like precipitate. This result can be understood by an overall increase in water content in the hydrogel due to the increase in hydration of MAA at basic pH, and is in agreement with DLS data that show that there is no variation in the size of the hydrogel with temperature. We must however assume that the hydrogen bonds of water with NIPAm are broken but the water content of the hydrogel is not changed by the water brought by the charged carboxylate groups. It is important to bear in mind that we are looking at the conformational freedom of methyl groups, which is largely affected by the dehydration of amide groups during NIPAm collapse. However, since they remain in an aqueous environment brought by the carboxylate groups, NIPAm collapse and the occurence of a VPT are largely prevented as we observe from DLS mesurements.

3.4. Impact of ionic strength on collapse

Experiments were performed at pH 6.8 at two different ionic strengths: 50 and 500 mM NaCl (Fig. 5). A more pronounced decrease in the intensity of the peak from the methyl protons than with acid pH can be observed with the ionic strength, up to 80% of the original signal. For both NaCl concentrations, the NMR signal decreased to the same final value intensity. However, the decrease in intensity is much faster for 500 mM (20 s, slope value 0.028) than for 50 mM (60 s, slope value 0.015). At the higher ionic strength we expect the hydrogel to be less hydrated at room temperature, which would account for the faster kinetics. Increasing ionic strength decreases the charge of the hydrogel and consequently the hydration of carboxylates. The ionic strength can also alter the hydraton shell around the NIPAm monomers, which may account for the more effective dehydration than with pH. Indeed, we observe a significant difference for the time at which the plateau starts between 50 and 500 mM NaCl, which must be associated with a lower phase transition temperature for 500 mM NaCl as it could be expected that the larger the salt concentration, the more the formation of hydrogen bonds between NIPAm and water molecules will be reduced. We cannot estimate in this case the temperature from the shifts of the methyl groups as the evolution of the chemical shifts with time does not follow the same trend as for the samples in D_2O and 50 mM NaCl (Fig. 5b, Fig. S6). The reason for the completely different chemical shift variation here is the modified temperature dependence of the chemical shift for D_2O due to the presence of a relatively large concentration of salt. In the case of 50 mM NaCl the shifts follow the same trend as D_2O without addition of NaCl. There is practically no shift for the temperature at which the plateau starts in 50 mM NaCl. Results at 500 mM NaCl may be affected by a change in the heat capacity of D_2O at this salt concentration. Further experiments are needed to have a clearer picture of the response of the hydrogels with high ionic strengths.

3.5. Interaction of hydrogels with doxorubicin, spermine/spermidine, and polyamines

P(NIPAm-*co*-MAA) hydrogels have potential applications in drug delivery of positively charged drugs, which can be complexed to carboxylate groups present in the hydrogel. Doxorubicin, a widely studied chemotherapeutic agent, is positively charged and can be encapsulated in the hydrogels by electrostatic interactions. We performed deswelling/swelling experiments with time-lapse NMR after doxorubicin encapsulation. In these experiments, neither the decay of intensity over time of the hydrogel nor the phase transition temperature are affected, indicating that doxorubicin does not change the hydration environment of the methyl groups of PNIPAm, and their rotational freedom is not affected (Fig. 6).

A very different situation is observed for spermidine and spermine, which are molecules of intermediate MW displaying 3 and

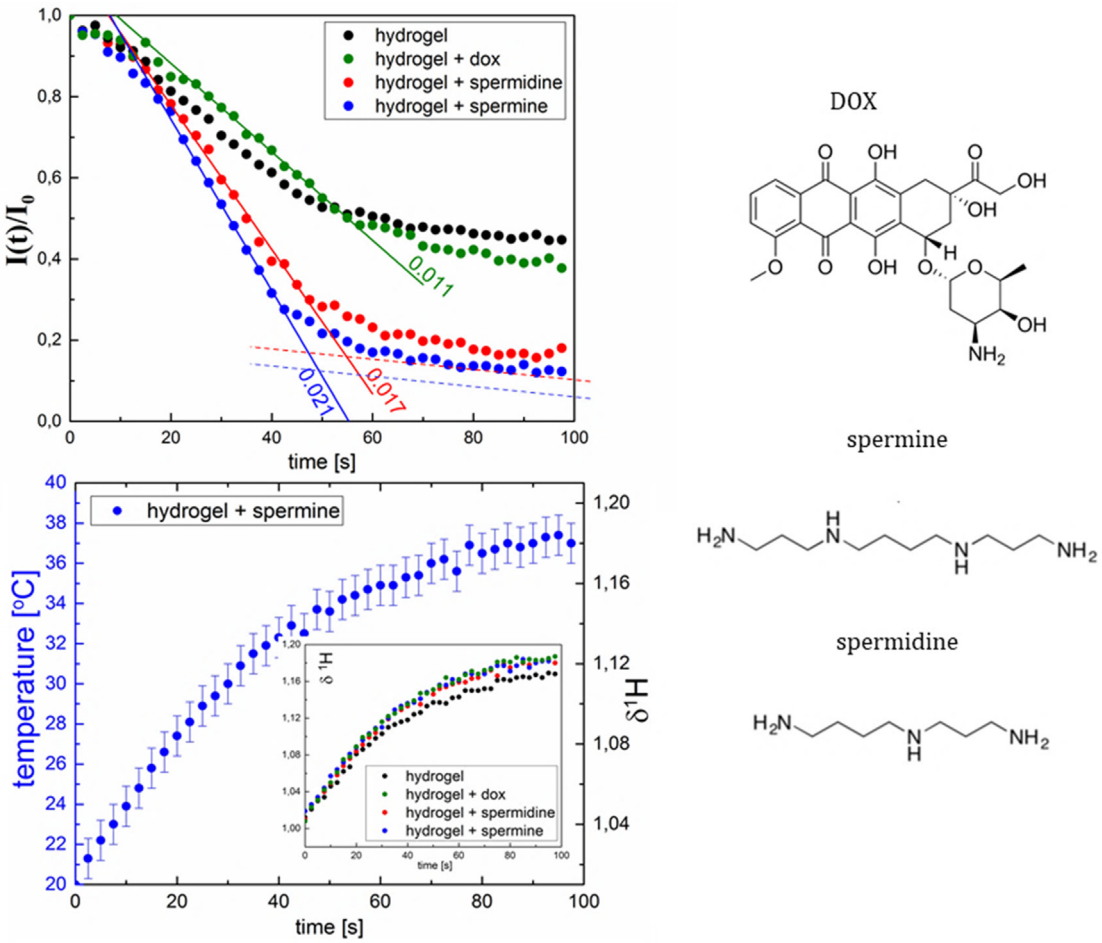

Fig. 6. Dehydration kinetics observed for PNIPAm microspheres in the presence of a small positively charged molecule (doxorubicin) and medium-sized oligomers (spermidine and spermine). Top, dotted lines show the evolution of the $I(t)/I_0$ of the methyl proton signal over time for the hydrogel alone, and in the presence of doxorubicin, spermidine and spermine. All experiments were recorded at pH 6.8. Bottom, temperature of the sample versus time for the hydrogel with spermine. The inset graph represents the chemical shift variation over time for all samples presented in top figure.

4 amine groups, respectively. These amine groups permit both spermidine and spermine to interact with more than one carboxylate group at the same time. Indeed, spermidine and spermine can complex several carboxylates restricting their mobility; however these molecules should not have a direct impact on the methyl groups of PNIPAm. Most likely the spermine and spermidine also have a dehydrating effect on the carboxylates, reducing water content in the hydrogel, and we cannot rule out the possibility that the amines of the two molecules do not form hydrogen bonds with NIPAm monomers, altering their mobility. Therefore, we observe a decrease of up to 80% of the original signal (Fig. 6, Fig. S7), comparable with the decrease in intensity seen when increasing the ionic strength. Spermine induces a slightly larger decrease in intensity than spermidine. This is probably due to the presence of one additional amine group in spermine which can link more carboxylate groups in the hydrogel resulting in effectively greater conformational freedom of the methyl group than spermidine. Practically no shift for the starting temperature of the plateau can be observed, which can be understood as none of the two molecules interacting directly with NIPAm and shoud not affect its interaction with water.

Furthermore, we performed time-lapse NMR after exposing the hydrogels to larger polyamines, PAH of two MWs, 15 kDa and 50 kDa, and PDADMAC in the same conditions described for DLS experiments. The addition of polycations displays abrupt dehydration kinetics for the systems studied (Fig. 7, Fig. S8). We have shown previously that polycations are very effective in dehydrating carboxylates [39]. However, it is only with PDADMAC that the decrease in NMR signal is as significant as that obtained for spermine and spermidine.

It is likely that the small polyamines (spermine/spermidine) are more effective at complexing carboxylate groups as they can penetrate more easily in the hydrogel and reach the hydrogel core. The larger polyamines (PAH, PDADMAC) are more likely to stay at least partially on the hydrogel surface due to molecular weight considerations [30]. Taking into account the MW of PDADMAC, we could expect that the polymer would remain predominantly on the surface of the hydrogel. However, in addition to a cross-complexation effect, quaternary ammoniums can generate a more hydrophobic environment than primary amines, which can lead to a decrease in the hydration of the carboxylates at room temperature as we have previously shown. This behaviour would explain why PDADMAC is more effective than PAH at decreasing the intensity of the NMR signal during hydrogel deswelling and consequently the conformational freedom of the methyl groups [36]. Despite the more pronounced decrease in intensity in the presence of PDADMAC, the temperature at which the plateau starts remains the same as for PAH, shifted anyway to lower values than the D_2O at pH 6.8. Probably, we observe here that both PAH and PDADMAC have a similar effect on the water environment around NIPAm, which determines the actual phase transition temperature.

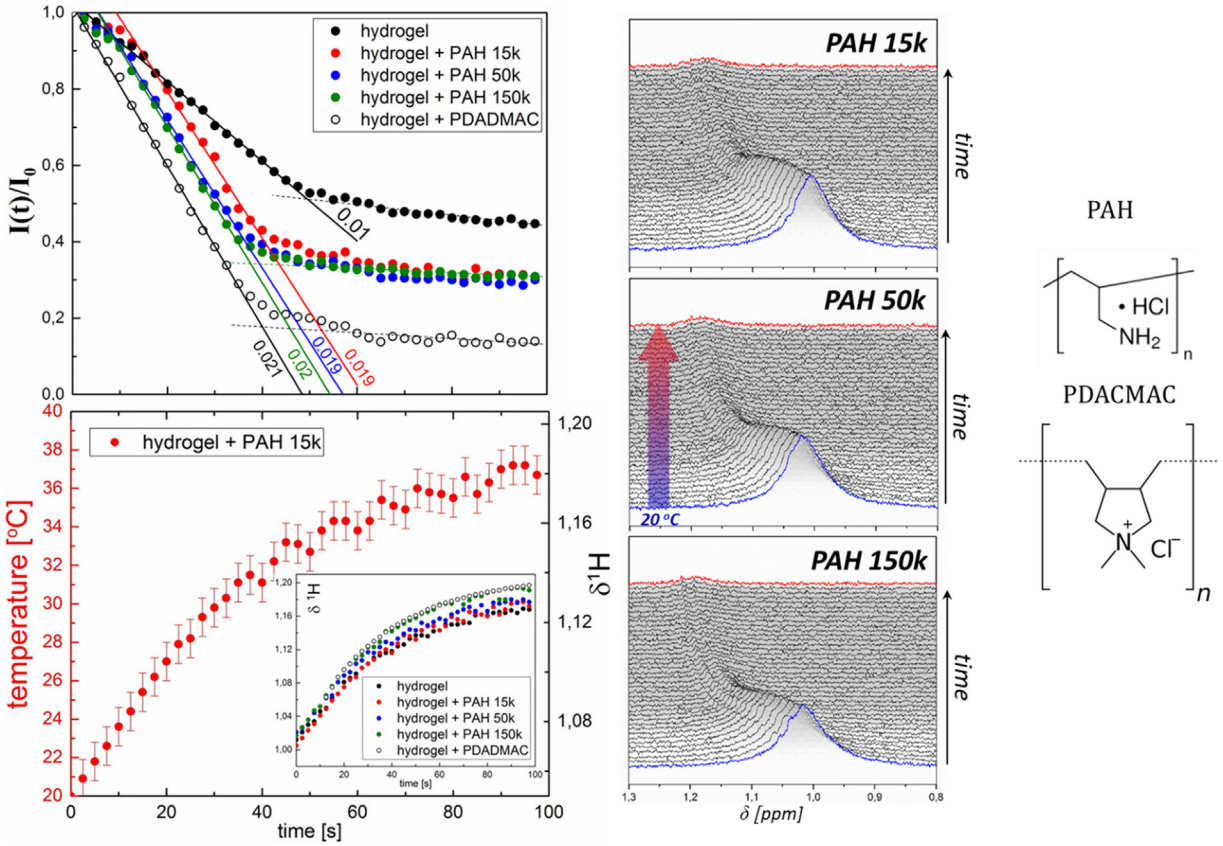

Fig. 7. Dehydration kinetics in the presence of PAH and PDADMAC. a) Evolution of the $I(t)/I_0$ over time for PAH of different MW and for PDADMAC. b) Temperature of the sample versus time for the hydrogel + PAH 15 k. The inset graph represents the chemical shift variation over time for PAH of different MW and for PDADMAC c) Change in the methyl proton NMR signal during deswelling for the three MWs of PAH studied. All experiments were recorded at pH 6.8.

4. Conclusions

Time-lapse NMR studies of P(NIPAm-*co*-MAA) hydrogels with temperature show a faster dehydration of the hydrogel at acid pH due to a decrease in the charge of carboxylates and water content. Notably, at basic pH no collapse can be inferred from the time-lapse NMR as the signal intensity is not affected by the increase in temperature. Although the hydrogen bonds of NIPAm with water are broken with temperature, the methyl groups of NIPAm remain in a highly hydrated environment due to the water brought by the carboxylates. Increasing the ionic strength results in faster dehydration kinetics as both carboxylate and PNIPAm groups dehydrate in the presence of NaCl below LCST. Positively charged oligomers, spermine and spermidine result in faster dehydration kinetics, which can be correlated with the oligomers complexing several carboxylate groups. Oligomers have a larger effect on the dehydration kinetics than PAH, probably due to a more effective penetration in the hydrogel, while PAH is largely retained on the hydrogel surface. PDADMAC, despite its high MW, shows dehydration kinetics similar to the oligomers because of the strong dehydrating effect of quaternary ammoniums on carboxylate groups [36]. Previous work has shown how the P(NIPAm-*co*-MAA) hydrogels respond to pH, exposure to polyamines [36] and temperature but without relating the temperature-induced swelling/deswelling of the hydrogel to the conformational freedom and hydration of NIPAm at the molecular level. Our results provide novel insight into these stimuli-induced responses of the hydrogel and give a molecular explanation for how the behavior of PNIPAm hydrogels is altered by the responsiveness of MAA monomers to the environment. Our time-lapse NMR experiments advance the understanding of the mechanism of collapse of P(NIPAm-*co*-MAA) hydrogels with temperature, and of how the sensitivity of MAA charges to various stimuli (pH, ionic strength, presence of charged molecules), can affect hydrogel collapse at the molecular level, which has not be demonstrated previously. This work opens new perspectives for using time-lapse NMR to study other hydrogels or smart thermoresponsive systems that respond to multiple stimuli, by examining the polymer dynamics in the hydrogel. Furthermore, time-lapse NMR has strong potential for studying the impact of molecular cargo in thermal transition for hydrogels designed for drug delivery.

CRediT authorship contribution statement

Marta Martinez-Moro: Methodology, Data curation, Investigation. **Jacek Jenczyk:** Investigation, Writing - original draft. **Juan M. Giussi:** Methodology, Investigation. **Stefan Jurga:** Conceptualization. **Sergio E. Moya:** Supervision, Investigation, Writing - review & editing.

Declaration of Competing Interest

The authors declare that they have no known competing financial interests or personal relationships that could have appeared to influence the work reported in this paper.

Acknowledgments

The research was supported by the H2020-INFRAIA-2016-2017 under research grant "EUSMI – European infrastructure for

spectroscopy, scattering and imaging of soft matter", contract number GA731019, funded under H2020-EU.1.4.1.2.–RIA. The authors thank the MAT2017-88752-R2017 Retos project from the Spanish Ministry of Economics. This work was performed under the Maria de Maeztu Units of Excellence Program from the Spanish State Research Agency – Grant No. MDM-2017-0720. We thank Julia Cope, PhD of CIC biomaGUNE for revising the manuscript and for useful suggestions.

Appendix A. Supplementary data

DLS of hydrogels in the presence of 20% PAH 15 kDa, 20% PAH 50 kDa, PDADMAC, spermine and spermidine; temperature dependance of HDO chemical shift; chemical shift variation observed for selected hydrogel samples; dehydration curves highlighting points chosen for lineal fiting and temperature evolution with time for dehydration curves. Supplementary data to this article can be found online at https://doi.org/10.1016/j.jcis.2020.07.049.

References

[1] L.A. Lyon, Z. Meng, N. Singh, C.D. Sorrell, A. St John, Thermoresponsive microgel-based materials, Chem. Soc. Rev. 38 (2009) 865–874, https://doi.org/10.1039/b715522k.
[2] F.A. Plamper, W. Richtering, Functional microgels and microgel systems, Acc. Chem. Res. 50 (2017) 131–140, https://doi.org/10.1021/acs.accounts.6b00544.
[3] H. Senff, W. Richtering, Temperature sensitive microgel suspensions: colloidal phase behavior and rheology of soft spheres, J. Chem. Phys. 111 (1999) 1705–1711, https://doi.org/10.1063/1.479430.
[4] H.G. Schild, Poly(N-isopropylacrylamide): experiment, theory and application, Prog. Polym. Sci. 17 (1992) 163–249, https://doi.org/10.1016/0079-6700(92)90023-R.
[5] W. Li, L. Hu, J. Zhu, D. Li, Y. Luan, W. Xu, M.J. Serpe, Comparison of the responsivity of solution-suspended and surface-bound poly(N-isopropylacrylamide)-based microgels for sensing applications, ACS Appl. Mater. Interfaces 9 (2017) 26539–26548, https://doi.org/10.1021/acsami.7b05558.
[6] D.S. Shin, E.Y. Tokuda, J.L. Leight, C.E. Miksch, T.E. Brown, K.S. Anseth, Synthesis of microgel sensors for spatial and temporal monitoring of protease activity, ACS Biomater. Sci. Eng. 4 (2018) 378–387, https://doi.org/10.1021/acsbiomaterials.7b00017.
[7] D. Buenger, F. Topuz, J. Groll, Hydrogels in sensing applications, Prog. Polym. Sci. 37 (2012) 1678–1719, https://doi.org/10.1016/j.progpolymsci.2012.09.001.
[8] J.P. Newsom, K.A. Payne, M.D. Krebs, Microgels: modular, tunable constructs for tissue regeneration, Acta Biomater. 88 (2019) 32–41, https://doi.org/10.1016/j.actbio.2019.02.011.
[9] M. Nakayama, T. Okano, T. Miyazaki, F. Kohori, K. Sakai, M. Yokoyama, Molecular design of biodegradable polymeric micelles for temperature-responsive drug release, J. Control. Release 115 (2006) 46–56, https://doi.org/10.1016/j.jconrel.2006.07.007.
[10] B. Sung, C. Kim, M.H. Kim, Biodegradable colloidal microgels with tunable thermosensitive volume phase transitions for controllable drug delivery, J. Colloid Interface Sci. 450 (2015) 26–33, https://doi.org/10.1016/j.jcis.2015.02.068.
[11] G. Fundueanu, M. Constantin, S. Bucatariu, P. Ascenzi, Poly(N-isopropylacrylamide-co-N-isopropylmethacrylamide) thermo-responsive microgels as self-regulated drug delivery system, Macromol. Chem. Phys. 217 (2016) 2525–2533, https://doi.org/10.1002/macp.201600324.
[12] M. Malmsten, H. Bysell, P. Hansson, Biomacromolecules in microgels — opportunities and challenges for drug delivery, Curr. Opin. Colloid Interface Sci. 15 (2010) 435–444, https://doi.org/10.1016/j.cocis.2010.05.016.
[13] N.M.B. Smeets, T. Hoare, Designing responsive microgels for drug delivery applications, J. Polym. Sci. Part A Polym. Chem. 51 (2013) 3027–3043, https://doi.org/10.1002/pola.26707.
[14] M.R. Matanović, J. Kristl, P.A. Grabnar, Thermoresponsive polymers: insights into decisive hydrogel characteristics, mechanisms of gelation, and promising biomedical applications, Int. J. Pharm. 472 (2014) 262–275, https://doi.org/10.1016/j.ijpharm.2014.06.029.
[15] T. Hoare, R. Pelton, Functional group distributions in carboxylic acid containing poly(N-isopropylacrylamide) microgels, Langmuir 20 (2004) 2123–2133, https://doi.org/10.1021/la0351562.
[16] B.R. Saunders, H.M. Crowther, B. Vincent, Poly[(methyl methacrylate)-co-(methacrylic acid)] microgel particles: swelling control using pH, cononsolvency, and osmotic deswelling, Macromolecules 30 (1997) 482–487, https://doi.org/10.1021/ma961277f.
[17] I.M. Okhapkin, I.R. Nasimova, E.E. Makhaeva, A.R. Khokhlov, Effect of complexation of monomer units on pH- and temperature-sensitive properties of poly(N-vinylcaprolactam-co-methacrylic acid), Macromolecules 36 (2003) 8130–8138, https://doi.org/10.1021/ma035114k.
[18] J.M. Giussi, M.I. Velasco, G.S. Longo, R.H. Acosta, O. Azzaroni, Unusual temperature-induced swelling of ionizable poly(N-isopropylacrylamide)-based microgels: experimental and theoretical insights into its molecular origin, Soft Matter 11 (2015) 8879–8886, https://doi.org/10.1039/C5SM01853F.
[19] J. Spěváček, Application of NMR Spectroscopy to Study Thermoresponsive Polymers, in: Temp. Polym., John Wiley & Sons Ltd, Chichester, UK, 2018: pp. 225–247. doi: 10.1002/9781119157830.ch9.
[20] J. Spěváček, R. Konefał, J. Dybal, E. Čadová, J. Kovářová, Thermoresponsive behavior of block copolymers of PEO and PNIPAm with different architecture in aqueous solutions: a study by NMR, FTIR, DSC and quantum-chemical calculations, Eur. Polym. J. 94 (2017) 471–483, https://doi.org/10.1016/j.eurpolymj.2017.07.034.
[21] R. Konefał, J. Spěváček, P. Černoch, Thermoresponsive poly(2-oxazoline) homopolymers and copolymers in aqueous solutions studied by NMR spectroscopy and dynamic light scattering, Eur. Polym. J. 100 (2018) 241–252, https://doi.org/10.1016/j.eurpolymj.2018.01.019.
[22] L. Loukotová, A. Bogomolova, R. Konefal, M. Špírková, P. Štěpánek, M. Hrubý, Hybrid κ-carrageenan-based polymers showing "schizophrenic" lower and upper critical solution temperatures and potassium responsiveness, Carbohydr. Polym. 210 (2019) 26–37, https://doi.org/10.1016/j.carbpol.2019.01.050.
[23] R. Konefał, J. Spěváček, E. Jäger, S. Petrova, Thermoresponsive behaviour of terpolymers containing poly(ethylene oxide), poly(2-ethyl-2-oxazoline) and poly(ε-caprolactone) blocks in aqueous solutions: an NMR study, Colloid Polym. Sci. 294 (2016) 1717–1726, https://doi.org/10.1007/s00396-016-3930-7.
[24] S.-H. Jung, H.-Y. Song, Y. Lee, H.M. Jeong, H.-I. Lee*, Novel thermoresponsive polymers tunable by pH, Macromolecules 44 (6) (2011) 1628–1634, https://doi.org/10.1021/ma102751p.
[25] A. Larsson, D. Kuckling, M. Schoenhoff, 1H NMR of thermoreversible polymers in solution and at interfaces: the influence of charged groups on the phase transition, Colloids and Surfaces A: Physicochemical and Engineering Aspects 190 (1–2) (2001) 185–192, https://doi.org/10.1016/S0927-7757(01)00678-1.
[26] F. Zeng, Zh.Tong H. Feng, N.m.r. investigation of phase separation in poly(N-isopropyl acrylamide)/water solutions Polymer 38, (1997), 5539-5544. doi: 10.1016/S0032-3861(97)00118-3.
[27] J.A. Yoon, C. Gayathri, R.R. Gil, T. Kowalewski, K. Matyjaszewski, Comparison of the thermoresponsive deswelling kinetics of poly(2-(2-methoxyethoxy)ethyl methacrylate) hydrogels prepared by ATRP and FRP, Macromolecules 43 (2010) 4791–4797, https://doi.org/10.1021/ma1004953.
[28] S. Sun, P. Wu, W. Zhang, W. Zhang, X. Zhu, Effect of structural constraint on dynamic self-assembly behavior of PNIPAM-based nonlinear multihydrophilic block copolymers, Soft Matter 9 (2013) 1807–1816, https://doi.org/10.1039/c2sm27183d.
[29] G. Ru, N. Wang, S. Huang, J. Feng, H HRMAS NMR study on phase transition of poly(N-isopropylacrylamide) gels with and without grafted comb-type chains, Macromolecules 42 (2009) 2074–2078, https://doi.org/10.1021/ma802780d.
[30] H. Tang, B. Zhang, P. Wu, On the two-step phase transition behavior of the Poly (N-isopropylacrylamide) (PNIPAM) brush: different zones with different orders, Soft Matter 10 (2014) 7278–7284, https://doi.org/10.1039/C4SM01182A.
[31] S. Zhou, B. Chu, Synthesis and volume phase transition of poly(methacrylic acid-co – N-isopropylacrylamide) microgel particles in water, J. Phys. Chem. B 102 (1998) 1364–1371, https://doi.org/10.1021/jp972990p.
[32] A.K. Bajpai, S.K. Shukla, S. Bhanu, S. Kankane, Responsive polymers in controlled drug delivery, Prog. Polym. Sci. 33 (2008) 1088–1118, https://doi.org/10.1016/j.progpolymsci.2008.07.005.
[33] J.M. Giussi, M. Martinez, A. Iborra, M.L. Cortez, D. Di Silvio, I. Llarena, G.S. Longo, O. Azzaroni, S.E. Moya, A study of the complex interaction between poly allylamine hydrochloride and negatively charged poly(N-isopropylacrylamide-co-methacrylic acid) microgels, Soft Matter 16 (2020) 881–890, https://doi.org/10.1039/C9SM02070E.
[34] K. Singh, E. Danieli, B. Blümich, Desktop NMR spectroscopy for real-time monitoring of an acetalization reaction in comparison with gas chromatography and NMR at 9.4 T, Anal. Bioanal. Chem. 409 (2017) 7223–7234, https://doi.org/10.1007/s00216-017-0686-y.
[35] M.V. Gomez, A. De La Hoz, NMR reaction monitoring in flow synthesis, Beilstein J. Org. Chem. 13 (2017) 285–300, https://doi.org/10.3762/bjoc.13.31.
[36] T. Tanaka, T. Amiya, A. Mamada, T. Tokuhiro, NMR study of poly(N-isopropylacrylamide) gels near phase transition, Macromolecules 24 (1991) 2936–2943, https://doi.org/10.1021/ma00010a046.
[37] G. Gao, M.A. Karaaslan, J.F. Kadla, F. Ko, Enzymatic synthesis of ionic responsive lignin nanofibres through surface poly(N-isopropylacrylamide) immobilization, Green Chem. 16 (2014) 3890–3898, https://doi.org/10.1039/c4gc00757c.
[38] H.E. Gottlieb, V. Kotlyar, A. Nudelman, NMR chemical shifts of common laboratory solvents as trace impurities, J. Org. Chem. 62 (1997) 7512–7515, https://doi.org/10.1021/jo971176v.
[39] T. Alonso, J. Irigoyen, J.J. Iturri, I.L. Larena, S.E. Moya, Study of the multilayer assembly and complex formation of poly(diallyldimethylammonium chloride) (PDADMAC) and poly(acrylic acid) (PAA) as a function of pH, Soft Matter 9 (2013) 1920–1928, https://doi.org/10.1039/C2SM26884A.